Volume 16, No 3 | International Journal of Radiation Research, July 2018

Evaluation of dosimetric characteristics of diodes and ionization chambers in small megavoltage photon field dosimetry

H. Keivan[1,2], D. Shahbazi-Gahrouei[1*], A. Shanei[1]

[1]Department of Medical Physics, School of Medicine, Isfahan University of Medical Sciences, Isfahan, Iran
[2]School of Paramedicine, Shahroud University of Medical Sciences, Shahroud, Iran

► ***Original article***

Corresponding authors:
Dr. D. Shahbazi-Gahrouei,
Fax: *+98 31 792 9032*
E-mail:
Shahbazi@med.mui.ac.ir

Revised: August 2017
Accepted: September 2017

Int. J. Radiat. Res., July 2018; 16(3): 311-321

DOI: 10.18869/acadpub.ijrr.16.3.311

ABSTRACT

Background: Modern radiation therapy such as intensity modulated radiation therapy (IMRT) and volumetric modulated arc therapy (VMAT) has resulted in using small therapeutic photon beams. The scope of this work is to investigate the variation in efficiency of different ionization chambers and semiconductor diodes in small multi-leaf collimator (MLC) defined fields of ARTISTE linear accelerator. ***Materials and Methods***: Dose distributions measurements was done in field sizes ranging from 0.5×0.5 to 10×10 cm^2 combining with Monte Carlo (MC) simulation. The treatment head of linac and the detectors were simulated by means of BEAMnrc/DOSXYZnrc of EGSnrc MC. The parameters such as output ratio (OR), penumbral width, dosimetric field size and the percentage surface dose in small radiation fields was evaluated using ionization chambers and semiconductor dosimeters. ***Results:*** ORs and beam profiles resulting from various measurements showed significant difference between ionization chambers and diodes in small fields. Derivation of less than 2% was observed between EDGE and Diode P. ORs vary by more than 30% for 1×1 cm2 field size but, in larger field sizes differences was less than 1%. Penumbra underestimation was seen in Semiflex relative to pinpoint ionization chamber. No difference was seen in the pattern of surface dose among the applied detectors. ***Conclusion:*** Dosimetric characteristics of different detectors showed significant differences in small photon beams. Profiles and ORs analysis with different dosimeters showed that not only water equivalency of detectors, but also dosimeter active volume is important factors for determination of dosimetric behavior in small photon beams.

Keywords: *Ionization chamber, diode, small field dosimetry.*

INTRODUCTION

With improvement of image guidance modality in modern radiation therapy techniques, traditional treatment radiation fields being reduced to small fields. Special treatment such as Stereotactic radiosurgery (SRS), volumetric modulated arc therapy (VMAT) and intensity modulated radiation therapy (IMRT) with small segments and narrow fields are successful in limiting damage to the normal tissues while delivering high doses of radiation to the target volumes [1]. In such superimposed small static or dynamic photon fields, because of nonstandard conditions that are related to both beam characteristics and the detector design, such as loss of lateral charged particle equilibrium (CPE) [2, 3], change in spectral photon fluence due to non-tissue equivalence of detectors [4], partial blocking of the x-ray source by the collimators [5, 6], penumbra overlapping [7] and stopping power ratios variations [8, 9], dosimetry is complicated and uncertain.

Dose calibration in reference dosimetry protocols such as IAEA TRS398 [10] and TG51 [11] depends on accurate dosimetric parameters and

beam quality. In ionization chambers absorbed dose to medium are calculated based on the cavity theory [2] and electronic equilibrium requirement in which the cavity size is smaller than the range of secondary charged particle passing it and fulfill CPE. In this conditions stopping power ratios determine the absorbed dose in the medium. But, in small fields the assumptions of cavity theory break down and CPE not provided, presence of detector cause perturbations (volume averaging effect) [12] and therefore, dosimetry in this fields strongly influenced by type and design of detector [13].

Particularly in IMRT where treatment fields include many small subfields, uncertainty in dosimetry data could enter into treatment planning system and affect in dose distribution and the accuracy of delivered dose to the target volume and organ at risks [7]. Therefore, the accurate measurement of dosimetric characteristic of small fields is an essential requirement. The selection of appropriate detector for dosimetry of small fields is challenging and in clinical practice it is necessary to choose suitable detector with best performance. Indeed, because of different collimation systems dose modeling in small fields in compare with large fields is complicated and affected by the MLC design [14].

The implementation of small megavoltage therapeutic photon beams requires careful assessment of dosimetry tools. Various manufactures provide ionization chambers and semiconductor diodes in different type and shape. But, there is no common agreement between researchers for the use of specific detector type.

Some studies have investigated the effect of construction and size of detectors in small radiation fields [15, 16]. Often of researchers have assessed the performance of various detectors in output factor measurements, but most of them limited their study in stereotactic radiation field produced by radiosurgery systems [17-23] and circular cones. Few studies focused on small field used in beamlets of linear accelerators. Many of IMRT fields use small segments shaped by MLCs of conventional linacs for dose delivery. In small fields collimated with MLCs, penumbra width of beam is clearly clinical significance and seems to be assessed along with output factors to evaluate performance of a detector.

Presently, national and international committees are working on dedicated dosimetry protocols for small field dosimetry.[24] The aim of this work is to evaluate the dosimetric characteristics of ionization chambers and semiconductor diodes in small megavoltage photon fields that can be used in commissioning of treatment planning systems. This work represents the capability of four ionization chambers with different volume and also three silicon diodes to measure MLC-defined small field output factors, as well as profiles and the percentage depth doses (PDDs).

MATERIALS AND METHODS

Measurements

In this work, four ionization chambers: Pinpoint (PTW-Freiburg, type 31006) Farmer (PTW-Freiburg, type 30013), Semiflex (PTW-Freiburg, type 31010) and Roos (PTW-34001) as well as three different semiconductor detectors: Diode E (60017), Diode P (60016) and EDGE (Sun Nuclear) were used for experimental measurements. Table 1, summarizes the main physical characteristic of the detectors used. All of experimental measurements were made in MP3 motorized water phantom (PTW-Freiburg) system (50 × 60 × 50 cm^3), a 3D scanning system that controlled by MEPHYSTO software. The positional accuracy of this water phantom based on manufacture data is 0.1 mm. Effective measurement point of detectors is adjusted at measurements depth using TrueFix system (PTW-Freiburg). To minimize the positional uncertainties in xy plane, using "Centerchek" module of MEPHYSTO software, zero point of radiation fields determined to a precision of ± 0.1 mm. This point is actual position of the central beam axis and was found by acquiring maximum signal of several off-axis profiles in cross plane and in planes. Detectors irradiation was carried out with ARTISTE™ medical linear accelerator

(Siemens, Medical Solutions) operating in x-ray mode 6 MV photons and dose rate 300 MU/min. The Artist single focused MLCs have equipped with 160 tungsten leaves that mounted in two leaf banks and each leaf has projected width of 5 mm at isocenter and allow 20 cm traveling and interdigitization. The maximum field resolution at isocenter is 0.5 × 0.5 cm^2.

For relative output factor ratio measurements, effective point of detectors placed at 10 cm depth in the water phantom. This depth was chosen because of contaminant electrons generated in accelerator head cannot propagate to the measurements points and perturb the dose results. The relative output ratio is defined as the ratio between electrometer readings for a specific field size in a particular depth and the reading for the reference field size (10 × 10 cm^2) at the same depth and same number of monitor units. Although RW3 slab phantoms could be used to relative output ratio measurements, the 3D system was preferred due to computerized controlling and ensure from accurate placement of the detectors. In the formalism for small field dosimetry introduced by Alfonso [4] the detector specific correction factor is applied to electrometer reading to account for detector material. But, in this study comparison between ionization chambers and semiconductor diode is done and output ratio measurements was referred.

The data was collected for the different nominal square field sizes of 0.5 × 0.5, 1 × 1, 1.5 × 1.5, 2 × 2, 2.5 × 2.5, 3 × 3, 4 × 4, 6 × 6 and 10 × 10 cm^2 at source to surface distance (SSD) of 100 cm. Each output factor ratio measurement was repeated three times and the averaged value normalized to the reference field size. The collimator jaws in y direction and MLCs in x direction collimated the radiation fields. All detectors were connected to the Unidos Universal electrometer (PTW-Freiburg) and manufacture recommended bios voltage was applied. All detectors were irradiated under 100 MU.

Measurement of the PDD was performed using four different detectors: the pinpoint ionization chamber, the Semiflex, the diode E and diode P. These detectors were used in conjunction with PTW MP3 water phantom and Tandem electrometer. The longitudinal dose distribution data along the beam axis from a depth of 30 cm to water surface were acquired for square field sizes of 10 × 10, 4 × 4, 3 × 3, 2 × 2 and 1 × 1 cm^2. The water phantom being set up at a SSD of 100 cm. Off-axis ratios (beam profiles) measurements were made to compare penumbra width for same field setting. Ionization chambers and EDGE detector were used in horizontal and other diodes in vertical orientation. Profile measurements were made in depth of 5 cm and for field sizes smaller than 4 cm^2 inter measurement spacing of 0.2 mm was used. All of relative measurement were made with gantry angle 0˚ and a dose rate of 300 MU min^{-1} and fixed measurement time of 0.1 s. The manufacture recommended bios voltage was applied in all cases. The linac was calibrated to deliver 1 cGy/MU at depth of maximum dose for field size 10 ×10 cm^2 and 100 cm SSD.

Monte Carlo simulations

Monte Carlo(MC) simulations is made by EGSnrc [25, 26] code packade (V4.2.4). Transporting of particle in the treatment head of linac (ARTISTE, 6 MV X-ray) was simulated using BEAMnrc according to the physical machine data and geometry provided by manufacturer. DOSXYZnrc was used to obtain the calculated dose distribution in phantom [27].

The electron beam incident on the target was assumed to be monoenergetic with a Guassian spatial distribution (ISOURCE=19). Therefore, initial beam parameters that influence the photon dose distribution are electron beam energy and radial intensity or full width at half maximum (FWHM) of the incident electrons.

To determine the optimum initial electron beam parameters in this study, the 6 MV photon beam was generated using a varying electron beam energy ranging from 5.9 MeV to 6.5 MeV in steps of 0.1 MeV incident on target and Guassian distribution characterized with FWHM equal 0.1 to 0.2 cm with 0.01 cm intervals. These two parameters were adjusted separately to obtain the best agreement between simulated and measured dose distribution. The total photon

and electron transport cut-offs energy (PCUT and ECUT) were set to 0.521 MeV and 0.01 MeV, respectively. Directional bremsstrahlung splitting (DBS) with 100 splitting number and range rejection with varying ECUTRR and ESAVE = 0.8 MeV was implemented as standard variance reduction techniques for avoid simulation of electrons that did not affect the phase space file significantly and improve the efficiency of simulation. To account for scatter into the field, the splitting radius was set to be 10 cm larger than the field sizes. The primary electron was set to 1.5×10^8 histories in BEAMnrc and the numbers of histories in the DOSXYZnrc input were assessed to produce a statistical uncertainty in calculated dose approximate 1%.

The field sizes varied between 1 × 1 to 10 × 10 cm^2 and phase space data was generated using BEAMnrc as a source file for DOSXYZnrc. The phase space files contain information about characteristic (charge, energy and direction) of particles on the scoring plane and scored below the linac MLCs. DOSXYZnrc was used to model the water phantom in which PDDs and dose profile is calculated. To model the detectors the method of Popescu [25] was used to simulate OR, and backscatter radiation to monitor chamber was not considered, as it was shown that have negligible effect in results.

The voxel dimension used for DOSXYZ calculation is set 0.1 × 0.1 × 0.1 cm^3 for penumbral region. Also, the voxel size of 0.2 × 0.2 × 0.1 cm^3 was used to calculate PDDs on central axis. For extract dose distribution data the EGSnrc utility program STATDOSE was used.

Table 1. Patient characteristics and scan parameters

Detector	Sensitive material	Inner electrode	Sensitive volume (mm^3)	Dimensions	Package Material
Semiflex (PTW-31010)	Air	Aluminum	125	5.5mm diameter, 6.5 mm lenght	Acrylic and graphite
Pinpoint (PTW-31016)	Air	Aluminum	16	2mm diameter, 5 mm lenght	Acrylic, graphite PMMA
Farmer (PTW-30013)	Air	Aluminum	600	6.2mm diameter, 23mm length	Graphite
ROOS (PTW-34001)	Air		350	15.6mm diameter	Graphite
Diode E (PTW-60012) Unshielded p-type	Silicon	-	0.03	1mm^2 front area 2.5 μm thickness	Epoxy resin and polymer plastic
Diode P (PTW6008) Shielded p-type	Silicon	-	0.03	1mm^2 front area 2.5 μm thickness	Epoxy resin and metal
EDGE (Sun Nuclear) Shielded n-type	Silicon	-	0.019	0.8mm length,0.03mm thickness	Brass

RESULTS

Validation of Monte Carlo simulation

Validation of MC simulation of linac head and fine tuning process was performed by comparison of measured and calculated dose distribution of 10 × 10 cm^2 field size. The FWHM and mean energy of the resultant incident Guassian intensity of electron beams were 0.15 cm and 6.2 MeV, respectively. Once the linac head had been fine-tuned, encompassing benchmarking was carried out by comparison of measured and calculated percentage depth dose and dose profiles in remaining field sizes.

Output ratios

OR analyze and comparison of ionization chambers and semiconductor diodes in 6 MV photon beam was done separately. Figure 1 demonstrates OR for each field width generated

by collimators and MLCs, normalized to a 10 × 10 cm^2 and measured by ionization chambers. This figure represents the ratio of electrometer reading without any correction factors. It is clear that in field sizes larger than 3 × 3 cm^2, the response of the Farmer and Roos chambers is approximately close to Pinpoint and Semiflex and negligible difference is seen between them.

OR measurement by semiconductor diodes illustrated in figure 2. As this figure shows, Diode P, Diode E and EDGE diode measure OR very close together in field sizes up to 4 × 4 cm^2. The agreement between EDGE and Diode P in OR measurements of field sizes below 4 × 4 cm^2 is smaller than 1%. Although in field sizes below 3 × 3 cm^2 large diversity is seen between EDGE and Diode E (2%-8%). For field sizes larger than 3 × 3 cm^2 lower difference between detectors was observed and maximum difference was smaller than 1%, while for field sizes smaller than 3 × 3 cm^2 there was higher discrepancy between detectors especially for field sizes smaller than 1 × 1 cm^2. With decrease in field size a steep drop in dose is observed for Farmer chamber.

The OR values obtained by Semiflex and Pinpoint chambers as well as diodes were compared with MC simulation and the percentage difference are summarized in figure 3. There is good agreement between Pinpoint detector and simulation with difference at the level of 1% for field sizes up to 3 × 3 cm^2. For fields smaller than 2 × 2 cm^2, the difference between the measured OR with diode detectors and the calculated OR, is smaller than the difference between that measured with ionization chambers and calculated by MC. Difference between Edge and Diode P with MC is less than 1.2% in small field sizes, while this value between small volume ionization chambers and MC reaches more than 30%.

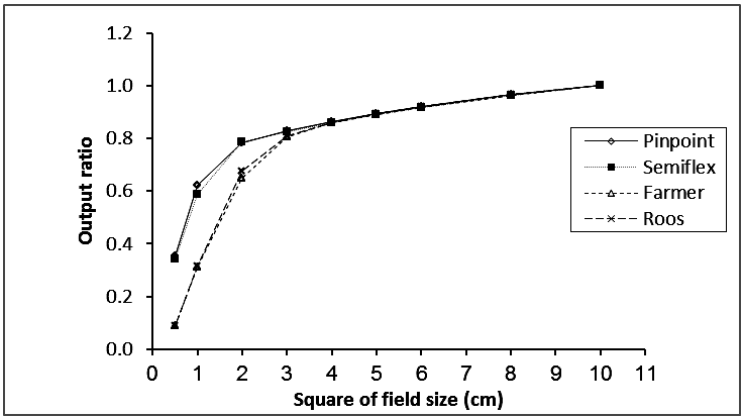

Figure 1. Comparison of output ratios in 6 MV photon fields measured with ionization chambers.

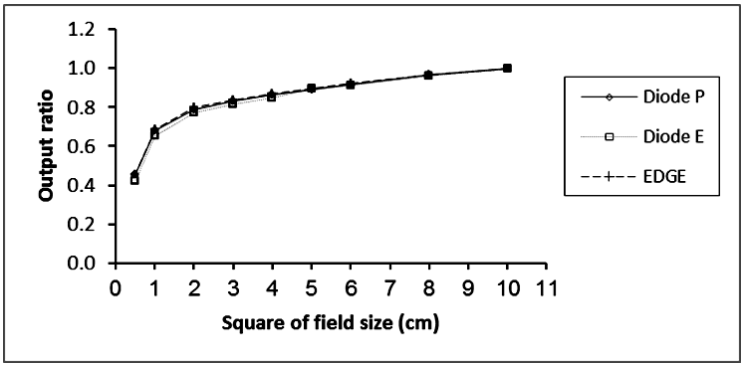

Figure 2. Comparison of output ratios in 6MV photon fields measured with diodes.

Penumbral region and field width

Steep dose gradient in the beam edge because of lateral electron disequilibrium results to penumbral region. The width of penumbra usually considered as lateral distance between 20% and 80% of isodose lines. The acquired profiles in depth 10 cm were normalized to 100% of central axis of beam for 1 × 1 to 10 × 10 cm^2 field sizes. The 80%-20% penumbra width for each detector and field size was measured and illustrated in figure 4. The greater field sizes, the increase in the penumbra region in all detectors were occurred.

The full width half maximum or dosimetric field size can be deduced by doubling of off axis distance of the minimum point of first derivation of each profile. This minimum point specifies the position of the maximum dose gradient for each field size. The value of maximum dose gradient is presented in table 2. Figure 5, represents relative difference between MC calculated field width and those measured by each detector.

Relative surface dose and depth dose at 10 cm

In general the measured PDD curves for all detectors are similar except in surface dose. Surface dose is important parameter yields an indication of the energy spectra and secondary charged particle produced in scattering materials in the path of X-ray photons [26] and therefore energy and field size dependent. Figure 6 shows the plot of percentage surface dose against field size for various detectors obtained from PDD curves. All detectors follow a similar pattern for different field size: for field sizes 3 × 3 cm^2 to 10 × 10 cm^2 percentage surface dose increase and for field sizes below 3 × 3 cm^2 a slight increase is seen in surface dose**.** The detector to detector variation in PDDs at depth 10 cm is illustrated in figure 7 for field sizes 1 × 1 to 10 × 10 cm^2. Despite relative surface dose, relative dose at 10 cm depth decrease with decreasing field size.

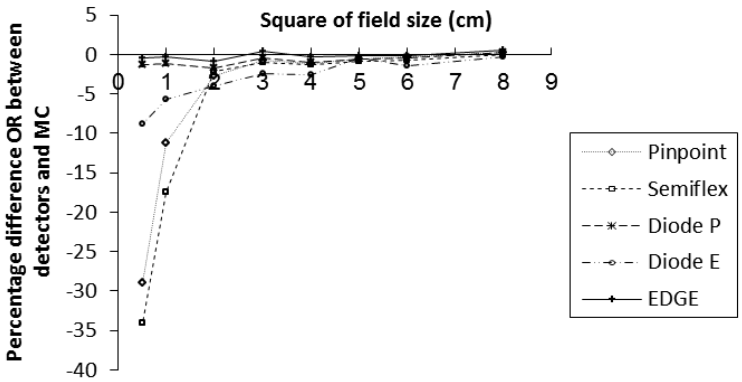

Figure 3. Percentage difference between output ratios calculated by MC and measured by each detector.

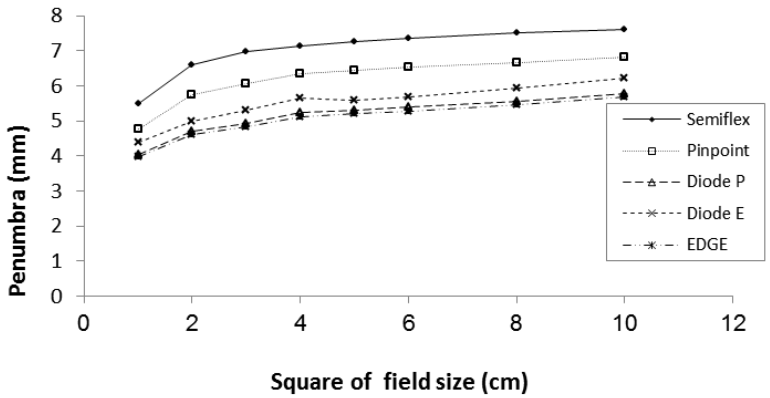

Figure 4. Comparison of penumbra width against field size with various detectors.

Table 1. Patient characteristics and scan parameters

Field size (cm^2)	Measured field size (cm)				
	Semiflex	Pinpoint	Diode P	Diode E	EDGE
1	1.173	1.121	1.081	1.112	1.069
2	2.068	2.077	2.064	2.101	2.040
3	3.114	3.124	3.108	3.142	3.065
4	4.161	4.164	4.147	4.178	4.100
5	5.208	5.213	5.193	5.217	5.135
6	6.254	6.247	6.233	6.256	6.135
8	8.350	8.342	8.325	8.349	8.245
10	10.442	10.431	10.385	10.404	10.300

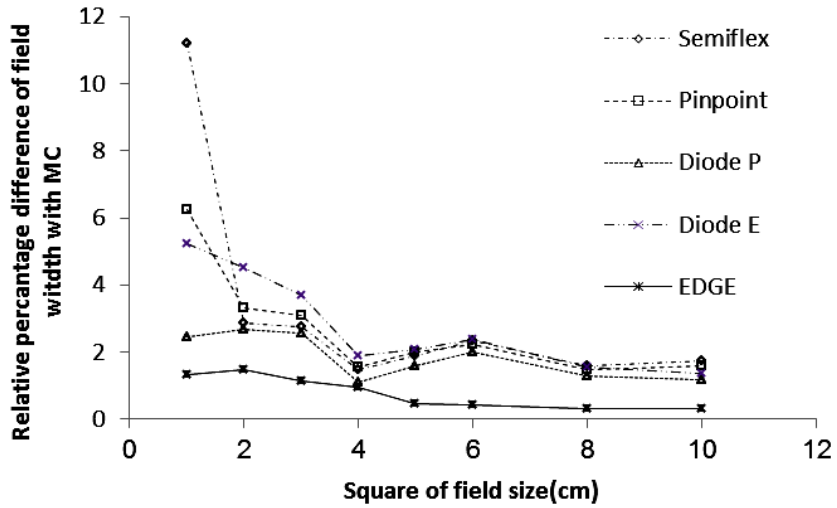

Figure 5. Relative percentage difference of field width calculated by MC and measured by various detectors.

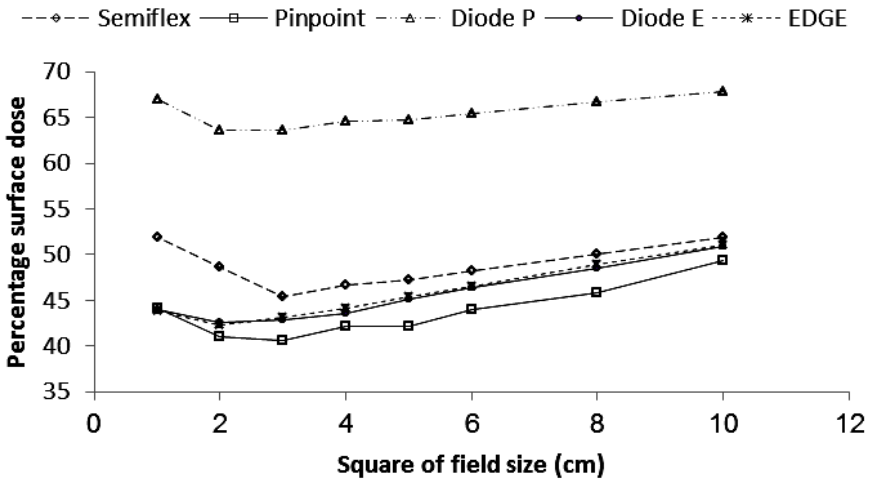

Figure 6. Comparison of percentage surface dose obtained by various detectors

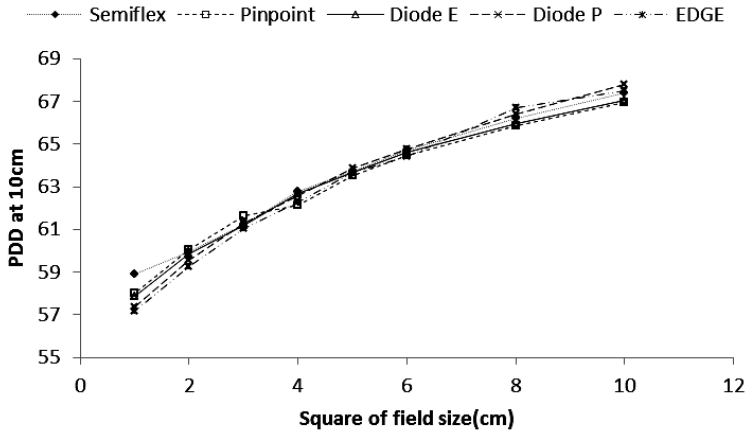

Figure 7. Comparison of PDD at 10 cm depth with various detectors.

DISCUSSION

Dose determination in small photon fields is an important and challenging task. Small photon fields are used in IMRT and VMAT, where MLCs create very small fields. In this work, the variation in efficiency of different ionization chambers and semiconductor diodes in small MLC defined fields of ARTISTE linear accelerator.

It implies that when lateral electronic equilibrium breaks down with decreasing field size, the active volume and water equivalency of the detector material become essential. From figure 1, it can be noted that for field sizes less than 3 × 3 cm^2, Farmer and Roos chambers underestimates ORs several percent than the values acquired with the other detectors. Comparison of air filled cavity of these chambers shows that size of air cavity has an important role in electronic disequilibrium and ORs estimation. The larger of air cavity size, the more decrease of CPE in small fields occurs and lower dose absorb in cavity with respect to water and results underestimation of ORs as reported in literature [20, 27]. The value of Pinpoint chamber has been investigated for small fields down to 2 cm^2 previously[38]. Results of this study showed that agreement between Pinpoint and Semiflex chambers is better than 0.5%, except for the field sizes below 1×1 cm^2 for which the volume averaging effect is predominant. Results of OPs are consistent with prior studies which have indicated that various detectors shows difference in output factor measurement with decreasing field size and variation rate are high for smallest field size [5, 7, 29-31].

Both air field ionization chambers and silicon diodes are not water equivalent however, comparison of detector materials between silicon and air showed that ORs measured by silicon diodes are closer to that measured by water voxel (figure 3). Decrease in field size to sub centimeters cause more electron disequilibrium in central axis of beam. But the lateral range of electrons in silicon is shorter than that in water and results a slower reduction of electron fluence in silicon diodes compared to air filled ionization chambers. Due to this effect, in small field sizes, the diode detectors yield closer response to MC in ORs as shown in figure 3. Francescon *et al.*[19] showed that small field detector specific correction factor for ionization chambers are 11% compared with 6% for diodes.

As reported in other study [32, 33] significant difference between detectors in penumbra measurements has been observed. Among various detectors used in this study, the broader penumbra obtained with the Semiflex ion chamber and narrowest belongs to semiconductor diodes. It is observed that ion chambers broaden the measured penumbra, while diode detectors provide rather accurate results. These data are agreement with those obtained by Bucciolini *et al* [34]. They showed that in small field sizes, measured penumbra by

RK ion chamber is 36% higher than those achieved by the diode detector. Another study have also been reported by Pappas *et al* [35]. reported that diodes' response is 56% higher than that Pinpoint in the smallest field size.

Penumbra broadening observed in ionization chambers is as a result of higher electron range in air than that in water. Instead, in silicon diodes, change of electron transport in silicon to water is quite less, therefore, semiconductor diodes yield narrowest penumbra. Ion chambers have more than 10% difference in penumbra measurements while Edge and Diode P have near approximation response (less than 2% difference). This is due to active volume of Pinpoint chamber that is eight times smaller than Semiflex chamber and volume averaging effect [36] outstanding. With decreasing field size, broadening effect is more enhanced. The comparison among these results reveals that penumbral width is influenced by both electron range alterations in different materials and volume averaging effect.

Results of table 2 reveal that the maximum difference with respect to nominal field size is seen in 1 × 1 field size for all detectors. In other field sizes this difference reduces about 4%. Diode P and EDGE have best estimation of field sizes with respect to other detectors. It can be understood from figure 5 that in small field sizes agreement between MC and diode detectors is better than MC and ionization chambers. In field sizes below 3 × 3 cm^2 all detector agree with MC in difference level of 2.5%. Difference is less than 1.5% is seen between simulation field width and EDGE detector in all field sizes. Especially for field sizes below 3 × 3 cm^2, maximum percentage difference between field width calculation and measurement belong to Semiflex (11%). It is predictable because Semiflex ion chamber has largest penumbra between all detectors.

Various types of detectors have been used to determination of surface dose of megavoltage photon beams. However, the results of this study consistent with previous measurements obtained by means of radiochromic film, thermoluminescense dosimeter and ionization chambers [37-39] that reported the increase of surface dose with increasing of field size for regular field sizes. But by decreasing field size (below 3×3 cm^2), surface doses slightly increase (figure 6) These measured values were in agreement with those calculated by means of Gafchromic EBT3 in small size fields[40].

It is seen from figure 6 that in field size of 10 × 10 the highest (67.88%) and lowest values (49.38%) for percentage surface dose belong to Diode P and Pinpoint respectively. Similar pattern for small field sizes is seen and maximum difference between two detectors is 36% occur in 3 × 3 cm^2 field size. The values obtained by Edge and diode E are similar in all field sizes and the comparison between two detectors shows that overall difference is less than 1.2%. These results are generally in accordance with other comparisons between silicon diodes and ionization chambers [34, 41].

The response of Diode P versus diamond detector in surface dose have also been reported by Scherf *et al.* [42] that showed that Diode P has 30% overestimation relative to diamond. In other study, Griessbach *et al.*[43] represented large surface dose of Diode P relative to thimble ionization chamber. The overestimation is related to the construction material of detector. Amount of high atomic number shielding metal placed at the surrounding of silicon, determinate amount of secondary scattered electrons to backslide. Therefore, in Diode P that silicon chip is partially encapsulated in a metal cap, scattering of secondary electrons in the metal and consequence their emission to backward is strong. This is the reason why the surface dose measured by Diode P is over estimated relative to other diode used in this work. This effect no has any difference between small and large fields and Diode P follow same manner for different field sizes. This effect has not any difference between small and large fields and Diode P follow same manner for different field sizes. This deficiency has been completely resolved in the case of Diode E and EDGE due to their constructions without a metallic shields.

Variation in PDDs at 10 cm depth (figure 7) illustrated that despite relative surface dose, relative dose at 10 cm depth decrease with decreasing field size. Negligible deviations

between detectors were seen for all field sizes and overall difference between maximum and minimum values in 1 × 1 cm^2 is less than 2.5% and in 10 × 10 cm^2 less than 1.2%.

CONCLUSION

Dosimetric characteristics of different detectors showed significant differences in small photon beams produced by linac MLCs. Profile and OR analysis with different dosimeters showed that not only water equivalency of detectors, but also dosimeter active volume is important factors for determination of dosimetric behavior of detectors in small photon beams. The sensitive volume effect of ionization chambers is more predominant than diodes and is a major factor in under responding of ion chambers in small field OR underestimation and penumbra broadening in small fields.

ACKNOWLEDGMENT

This work is a part of PhD thesis which financially supported by Isfahan University of Medical Sciences (Grant No. 394427).

***Conflicts of interest*: Declared none.**

REFERENCES

1. Cyriac T, Musthafa M, Ganapathi Raman R, Abdul Haneefa K, Saju B (2015) Out-of-field photon dosimetry study between 3-D conformal and intensity modulated radiation therapy in the management of prostate cancer. *Int J Radiat Res, **13(2)**: 127-134*
2. Shahbazi-Gahrouei D, Saeb, M, Monadi S, Jabbari I (2017) Clinical implications of TiGRT algorithm for external audit in radiation oncology. *Adv Biomed Res; 6, 117.*
3. Sharma S (2014) Challenges of small photon field dosimetry are still challenging. Journal of *Medical Physics, **39(3)**: 131.*
4. Alfonso R, Andreo P, Capote R, Huq MS, Kilby W, Kjäll P, *et al.* (2008) A new formalism for reference dosimetry of small and nonstandard fields. *Med Phys*, **35(11)**: 5179-5186.*
5. Tyler M, Liu PZ, Chan KW, Ralston A, McKenzie DR, Downes S, *et al.* (2013) Characterization of small-field stereotactic radiosurgery beams with modern detectors. *Phys Med Biol*, **58(21)**: 7595-7608.*
6. Khosravi M, Shahbazi-Gahrouei D, Jabbari K, Baradaran-Ghahfarokhi M, Gheisari R, Amiri B (2013) Photoneutron contamination from an 18 MV Saturne Medical Linear Accelerator in treatment room: Monte-Carlo simulation. *Radiat Protec Dosimetry*, **156(3)**: 356-363.*
7. Rezaee V, Shahbazi-Gahrouei D, Monadi S, Saeb M (2016) Evaluation of error doses of treatment planning software using solid Anthropomorphic phantom. *J Isfahan Med Sch, **34(393)**: 908-913.*
8. Sánchez-Doblado F, Andreo P, Capote R, Leal A, Perucha M, Arráns R, *et al.* (2003) Ionization chamber dosimetry of small photon fields: A Monte Carlo study on stopping-power ratios for radiosurgery and IMRT beams. *Phys Med Biol*, **48(14)**: 2081-2099.
9. Mosleh-Shirazi MA, Karbasi S, Shahbazi-Gahrouei D, Monadi S (2012) A Monte Carlo and experimental investigation of the dosimetric behavior of low-and medium-perturbation diodes used for entrance in vivo dosimetry in megavoltage photon beams. *J Appl Clinical Med Phys, **13(6)**: 326-338.*
10. Shahbazi-Gahrouei D, Baradaran-Ghahfarokhi M (2013) Assessment of entrance surface dose and health risk from common radiology examinations in Iran. *Radiat Protec Dosimetry*, **154**: 308-313.*
11. Almond PR, Biggs PJ, Coursey BM, Hanson WF, Huq MS, Nath R, *et al.* (1999) AAPM's TG-51 protocol for clinical reference dosimetry of high-energy photon and electron beams. *Med Phys*, **26(9)**: 1847-1870.*
12. Laub WU and Wong T (2003) The volume effect of detectors in the dosimetry of small fields used in IMRT. *Med Phys, **30**: 341-347.*
13. Cyarnecki D and Zink K (2013) Monte Carlo calculated correction factors for diodes and ion chambers in small photon fields. *Phys Med Biol, **58**: 2431–2444.*
14. Lydon J (2005) Theoretical and experimental validation of treatment planning for narrow MLC defined photon fields. *Phys Med Biol*, **50(11)**: 2701.*
15. Scott AJ, Kumar S, Nahum AE, Fenwick JD (2012) Characterizing the influence of detector density on dosimeter response in non-equilibrium small photon fields. *Phys Med Biol*, **57(14)**: 4461.*
16. Underwood T, Winter H, Hill M, Fenwick J (2013) Detector density and small field dosimetry: integral versus point dose measurement schemes. *Med Phys*, **40(8)**: 082102.*
17. Francescon P, Cora S, Cavedon C (2008) Total scatter factors of small beams: a multidetector and Monte Carlo study. *Med Phys*, **35(2)**: 504-513.*
18. Manolopoulos S, Wojnecki C, Hugtenburg R, Sidek MJ, Chalmers G, Heyes G, *et al.* (2009) Small field measurements with a novel silicon position sensitive diode array. *Phys Med Biol, **54(3)**: 485.*
19. Francescon P, Kilby W, Satariano N, Cora S (2012) Monte Carlo simulated correction factors for machine specific

reference field dose calibration and output factor measurement using fixed and iris collimators on the CyberKnife system. *Phys Med Biol*, ***57(12)****: 3741-3758.*

20. Araki F (2006) Monte Carlo study of a Cyberknife stereotactic radiosurgery system. *Med Phys*, ***33(8)****: 2955-2963.*
21. Dieterich S and Sherouse GW (2011) Experimental comparison of seven commercial dosimetry diodes for measurement of stereotactic radiosurgery cone factors. *Med Phys,* ***38(7)****: 4166-4173.*
22. Azangwe G, Grochowska P, Georg D, Izewska J, Hopfgartner J, Lechner W, *et al.* (2014) Detector to detector corrections: a comprehensive experimental study of detector specific correction factors for beam output measurements for small radiotherapy beams. *Med Phys,****41(7)****: 072103.*
23. Benmakhlouf H, Johansson J, Paddick I, Andreo P (2015) Monte Carlo calculated and experimentally determined output correction factors for small field detectors in Leksell Gamma Knife Perfexion beams. *Phys Med and Biol*, ***60(10)****: 3959.*
24. Yarahmadi M, Nedaie H, Allahverdi M, Asnaashari K, Sauer O (2013) Small photon field dosimetry using EBT2 Gafchromic film and Monte Carlo simulation. *Int J Radiat Res,* ***11(4)****: 215-224.*
25. Popescu IA, Shaw CP, Zavgorodni SF, Beckham WA (2005) Absolute dose calculations for Monte Carlo simulations of radiotherapy beams. *Phys Med Biol,* ***50(14)****: 3375-3392.*
26. Karbalee M, Shahbazi-Gahrouei D, Tavakoli MB (2017) An approach in radiation therapy treatment planning: A fast GPU-based Monte Carlo method. *J Med Signals Sens*, ***7(2)****: 108-113*.
27. Lauba WU and Wong T (2003) The volume effect of detectors in the dosimetry of small fields used in IMRT. *Med Phys,* ***30(3)****: 341-347.*
28. Martens C, De Wagter C, De Neve W (2000) The value of the PinPoint ion chamber for characterization of small field segments used in intensity-modulated radiotherapy. *Phys Med Biol,* ***45(9)****: 2519.*
29. Rogers D, Walters B, Kawrakow I (2009) BEAMnrc users manual. *NRC Report PIRS,* ***509****: 12.*
30. Keivan H, Shahbazi-Gahrouei D, Shanei A, Amouheidari A (2018) Assessment of Imprecise Small Photon Beam Modeling by Two Treatment Planning System Algorithms. Journal of Medical Signals and Sensors. ***8(1):****39-45.*
31. Bassinet C, Huet C, Derreumaux S, Brunet G, Chéa M, Baumann M, *et al.* (2013) Small fields output factors measurements and correction factors determination for several detectors for a CyberKnife® and linear accelerators equipped with microMLC and circular cones. *Med Phys,* ***40 (7)****: 071725.*
32. Chang KS, Yin FF, Nie KW (1996) The effect of detector size to the broadening of the penumbra- a computer simulated study. *Med Phys,* ***23(8)****: 1407-1411.*
33. Kang SW, Chung JB, Lee JW, Kim MJ, Kim YL, Kim JS, *et al.* (2017) Dosimetric accuracy of the Acuros XB and Anisotropic analytical algorithm near interface of the different density media for the small fields of a 6- MV flattening-filter-free beam. *Int J Radiat Res,* ***15(2)****: 157-165.*
34. Bucciolini M, Banci Buonamici F, Mazzocchi S, De Angelis C, Onori S, Cirrone G (2003) Diamond detector versus silicon diode and ion chamber in photon beams of different energy and field size. *Medical Phys,* ***30(8)****: 2149-2154.*
35. Pappas E, Maris T, Zacharopoulou F, Papadakis A, Manolopoulos S, Green S, *et al.* (2008) Small SRS photon field profile dosimetry performed using a PinPoint air ion chamber, a diamond detector, a novel silicon-diode array (DOSI), and polymer gel dosimetry. Analysis and intercomparison. *Med Phys,* ***35(10)****: 4640-4648.*
36. Pappas E, Maris T, Papadakis A, Zacharopoulou F, Damilakis J, Papanikolaou N, *et al.* (2006) Experimental determination of the effect of detector size on profile measurements in narrow photon beams. *Med Phys,* ***33 (10)****: 3700-3710.*
37. Bilge H, Ozbek N, Okutan M, Cakir A, Acar H (2010) Surface dose and build-up region measurements with wedge filters for 6 and 18 MV photon beams. *Japanese J Radiol,* ***28(2)****: 110-116.*
38. Stathakis S, Li J, Paskalev K, Yang J, Wang L, Ma C (2006) Ultra-thin TLDs for skin dose determination in high energy photon beams. *Phys Med Biol,* ***51(14)****: 3549.*
39. Chen F, Gupta R, Metcalfe P (2010) Intensity modulated radiation therapy (IMRT) surface dose measurements using a PTW advanced Markus chamber. *Australas Phys Eng Sci Med,* **33(1)**: 23-34.
40. Morales J, Hill R, Crowe S, Kairn T, Trapp J (2014) A comparison of surface doses for very small field size x-ray beams: Monte Carlo calculations and radiochromic film measurements(2014). *Australas Phys Eng Sci Med,* ***37(2)****: 303-309.*
41. Djouguela A, Grießbach I, Harder D, Kollhoff R, Chofor N, Rühmann A, *et al.* (2008). Dosimetric characteristics of an unshielded p-type Si diode: linearity, photon energy dependence and spatial resolution. *Zeitschrift für Medizinische Physik,* ***18(4)****: 301-306.*
42. Scherf C, Peter C, Moog J, Licher J, Kara E, Zink K, *et al.* (2009) Silicon diodes as an alternative to diamond detectors for depth dose curves and profile measurements of photon and electron radiation. *Strahlentherapie und Onkologie,* ***185(8)****: 530-536.*
43. Griessbach I, Lapp M, Bohsung J, Gademann G, Harder D (2005) Dosimetric characteristics of a new unshielded silicon diode and its application in clinical photon and electron beams. *Med Phys,* ***32(12)****: 3750-3754.*